University of Zurich[UZH]

Zurich Open Repository and Archive
University of Zurich
University Library
Strickhofstrasse 39
CH-8057 Zurich
www.zora.uzh.ch

Year: 2013

Sulfatides are required for renal adaptation to chronic metabolic acidosis

Stettner, Paula ; Bourgeois, Soline ; Marsching, Christian ; Traykova-Brauch, Milena ; Porubsky, Stefan ; Nordström, Viola ; Hopf, Carsten ; Kösters, Robert ; Sandhoff, Roger ; Wiegandt, Herbert ; Wagner, Carsten A ; Gröne, Hermann-Josef ; Jennemann, Richard

Abstract: Urinary ammonium excretion by the kidney is essential for renal excretion of sufficient amounts of protons and to maintain stable blood pH. Ammonium secretion by the collecting duct epithelia accounts for the majority of urinary ammonium; it is driven by an interstitium-to-lumen NH3 gradient due to the accumulation of ammonium in the medullary and papillary interstitium. Here, we demonstrate that sulfatides, highly charged anionic glycosphingolipids, are important for maintaining high papillary ammonium concentration and increased urinary acid elimination during metabolic acidosis. We disrupted sulfatide synthesis by a genetic approach along the entire renal tubule. Renal sulfatide-deficient mice had lower urinary pH accompanied by lower ammonium excretion. Upon acid diet, they showed impaired ammonuria, decreased ammonium accumulation in the papilla, and chronic hyperchloremic metabolic acidosis. Expression levels of ammoniagenic enzymes and Na(+)-K(+)/NH4(+)-2Cl(-) cotransporter 2 were higher, and transepithelial NH3 transport, examined by in vitro microperfusion of cortical and outer medullary collecting ducts, was unaffected in mutant mice. We therefore suggest that sulfatides act as counterions for interstitial ammonium facilitating its retention in the papilla. This study points to a seminal role of sulfatides in renal ammonium handling, urinary acidification, and acid-base homeostasis.

DOI: https://doi.org/10.1073/pnas.1217775110

Posted at the Zurich Open Repository and Archive, University of Zurich
ZORA URL: https://doi.org/10.5167/uzh-79448
Journal Article
Accepted Version

Originally published at:
Stettner, Paula; Bourgeois, Soline; Marsching, Christian; Traykova-Brauch, Milena; Porubsky, Stefan; Nordström, Viola; Hopf, Carsten; Kösters, Robert; Sandhoff, Roger; Wiegandt, Herbert; Wagner, Carsten A; Gröne, Hermann-Josef; Jennemann, Richard (2013). Sulfatides are required for renal adaptation to chronic metabolic acidosis. Proceedings of the National Academy of Sciences of the United States of America, 110(24):9998-10003.
DOI: https://doi.org/10.1073/pnas.1217775110

SUPPORTING FIGURES AND FIGURE LEGENDS

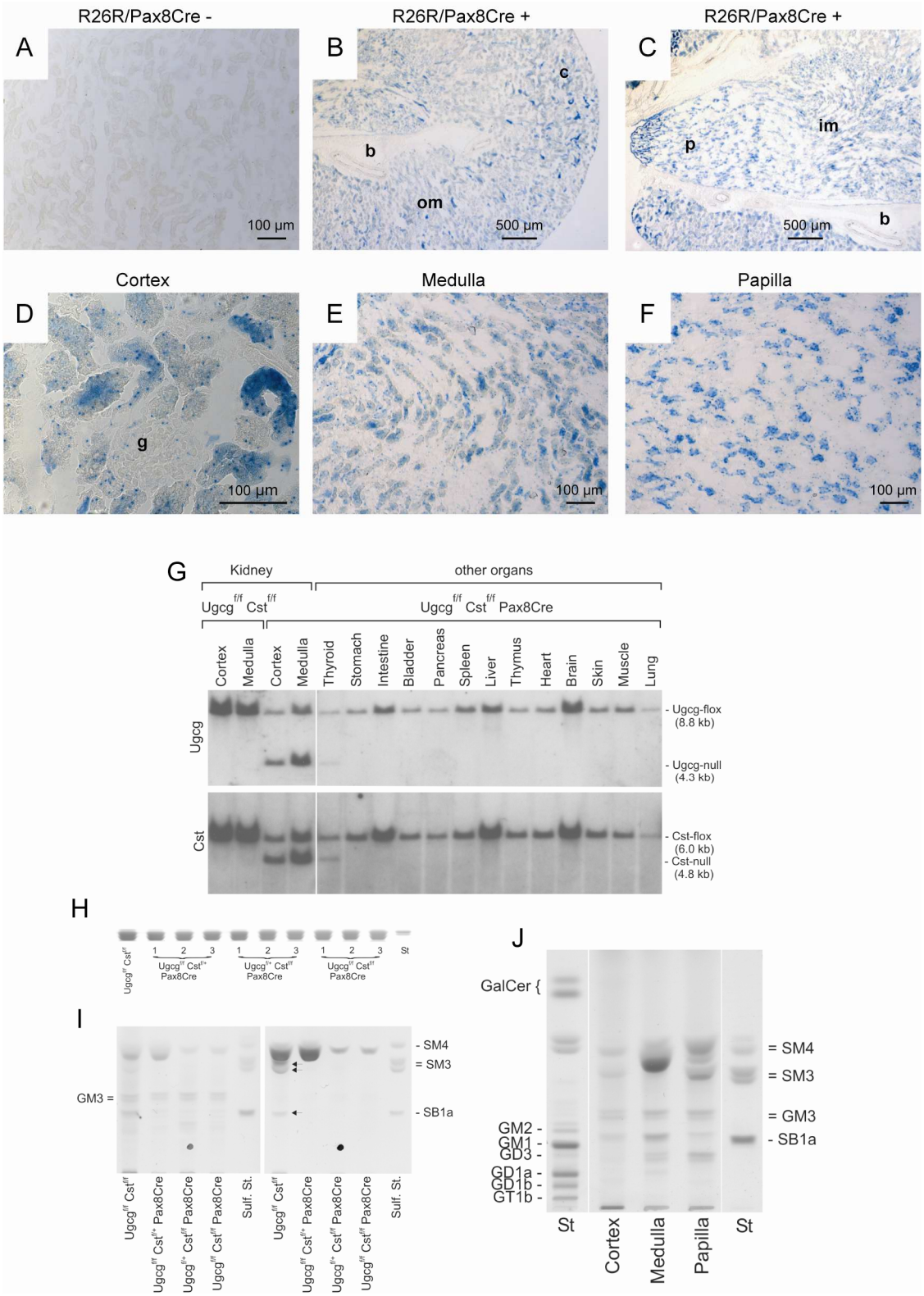

Fig. S1

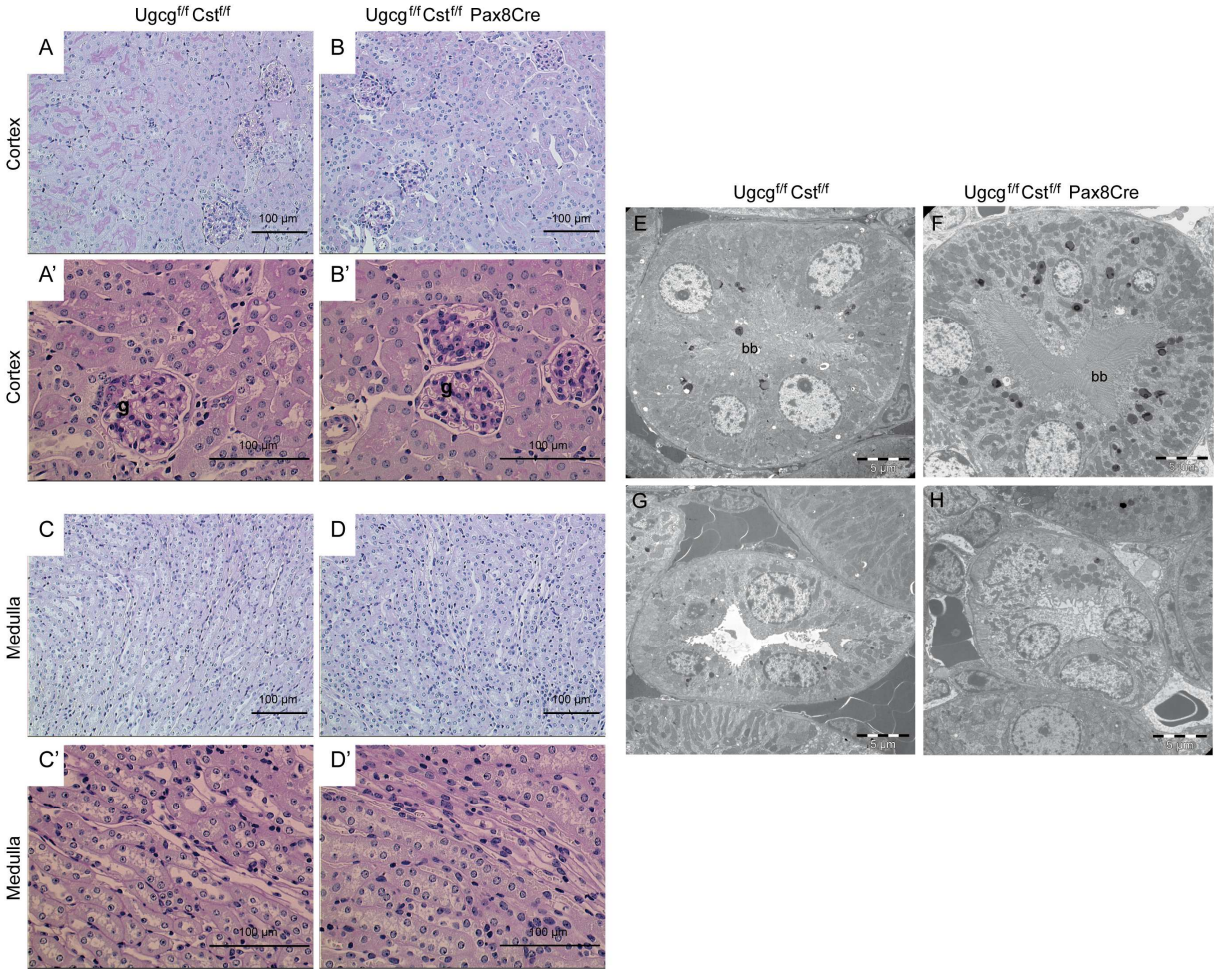
Ugcg f/f Cst f/f
Ugcg f/f Cst f/f Pax8Cre
A
B
Cortex
100 µm
A'
B'
Cortex
g
C
D
Medulla
C'
D'
Medulla
Ugcg f/f Cst f/f
Ugcg f/f Cst f/f Pax8Cre
E
F
bb
5 µm
G
H

Fig. S2

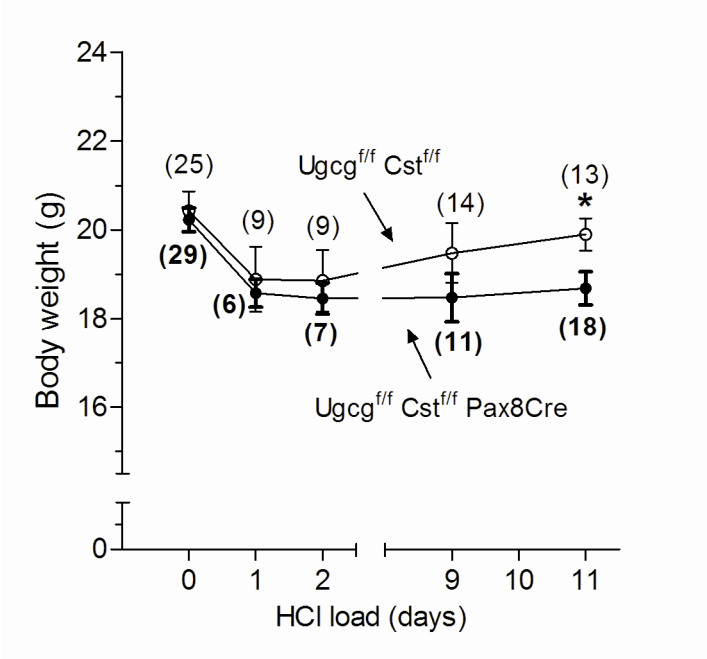
Body weight (g)
24
22
20
18
16
0
(25)
(29)
(9)
(6)
(9)
(7)
(14)
(11)
(13)
*
(18)
Ugcg f/f Cst f/f
Ugcg f/f Cst f/f Pax8Cre
0
1
2
9
10
11
HCl load (days)

Fig. S3

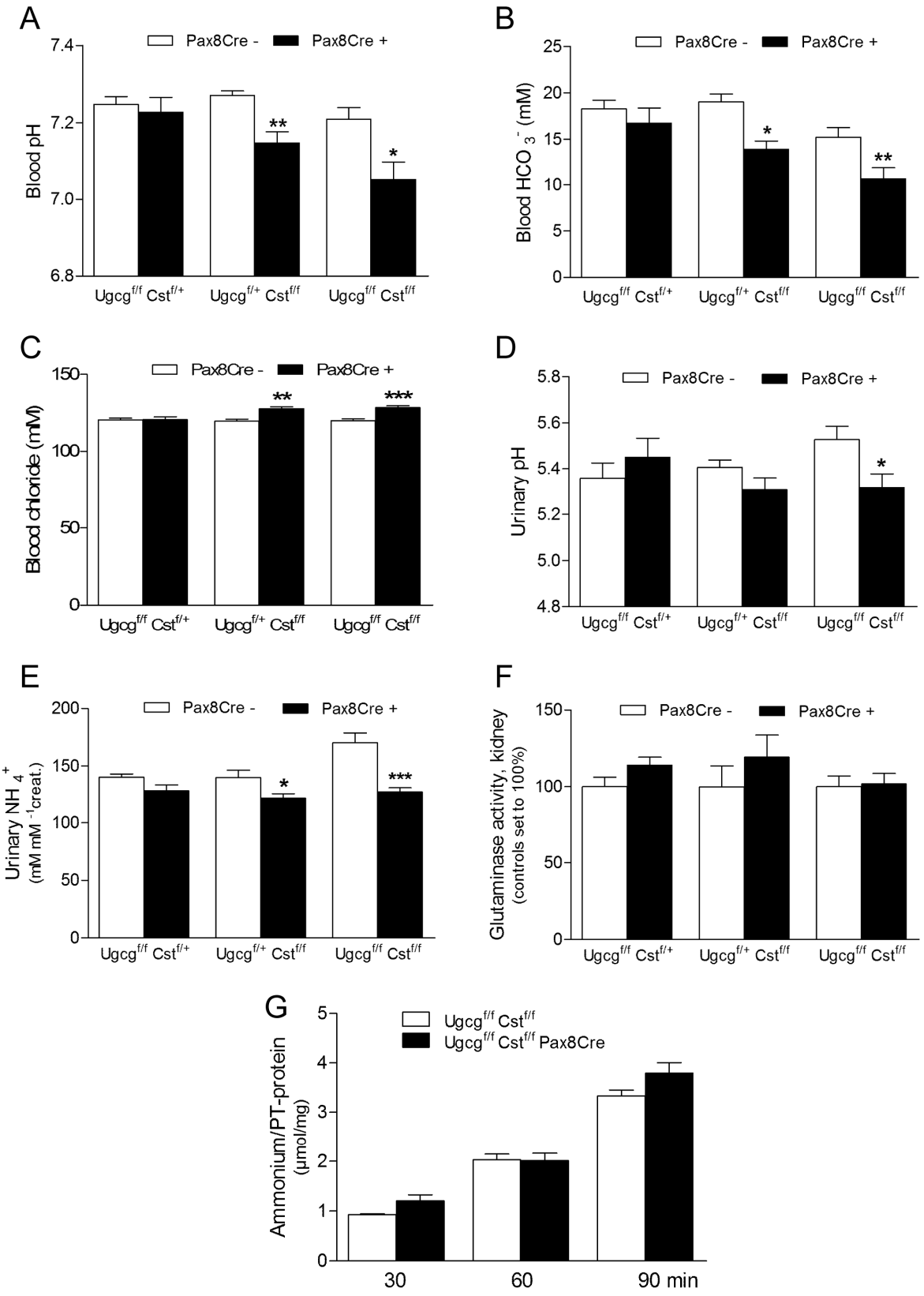
A
Pax8Cre -
Pax8Cre +
Blood pH
7.4
7.2
7.0
6.8
**
*
Ugcg f/f Cst f/+
Ugcg f/+ Cst f/f
Ugcg f/f Cst f/f
B
Blood HCO 3 - (mM)
25
20
15
10
5
0
*
**
C
Blood chloride (mM)
150
100
50
0
**
***
D
Urinary pH
5.8
5.6
5.4
5.2
5.0
4.8
*
E
Urinary NH 4 +
(mM mM -1creat.)
200
150
100
50
0
*
***
F
Glutaminase activity, kidney
(controls set to 100%)
150
100
50
0
G
Ugcg f/f Cst f/f
Ugcg f/f Cst f/f Pax8Cre
Ammonium/PT-protein
(µmol/mg)
5
4
3
2
1
0
30
60
90 min

Fig. S4

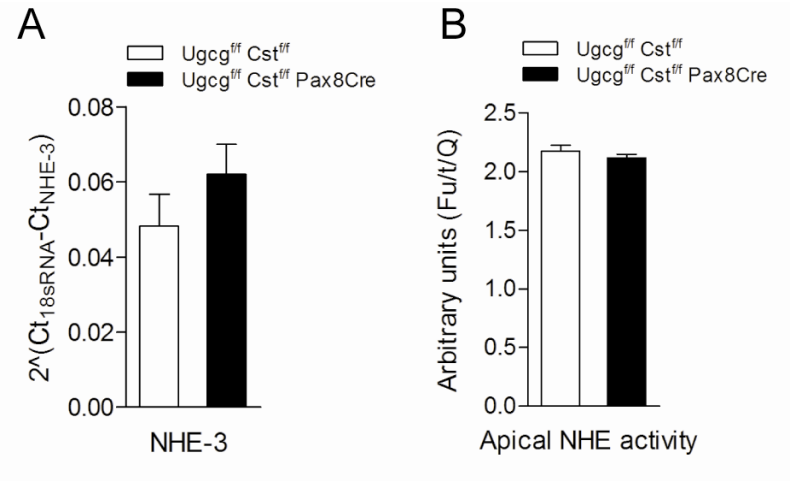
A
Ugcg^f/f Cst^f/f
Ugcg^f/f Cst^f/f Pax8Cre
0.08
0.06
0.04
0.02
0.00
2^(Ct18sRNA-CtNHE-3)
NHE-3
B
Ugcg^f/f Cst^f/f
Ugcg^f/f Cst^f/f Pax8Cre
2.5
2.0
1.5
1.0
0.5
0.0
Arbitrary units (Fu/t/Q)
Apical NHE activity

Fig. S5

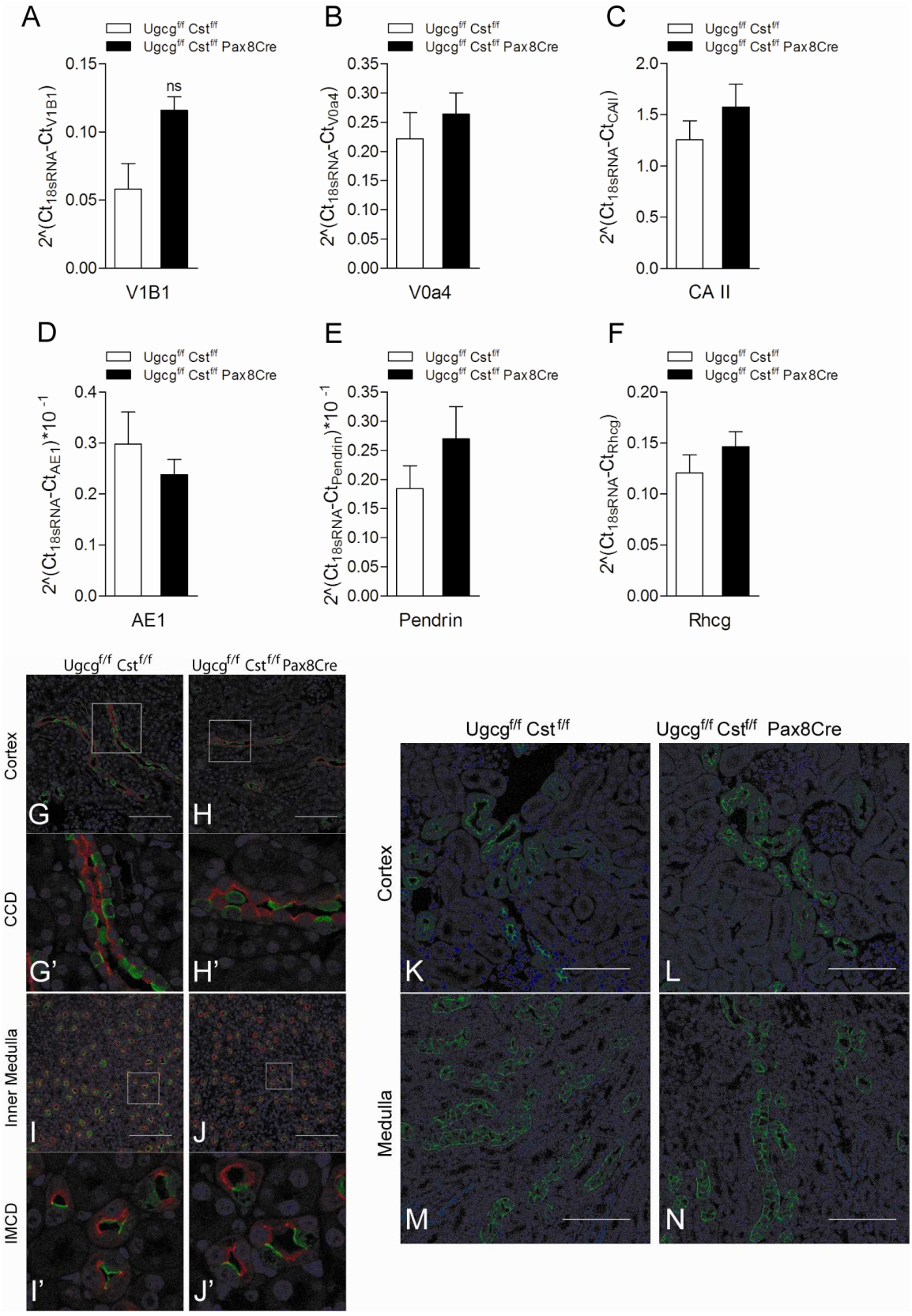
A
B
C
D
E
F
Ugcg f/f Cst f/f
Ugcg f/f Cst f/f Pax8Cre
ns
V1B1
V0a4
CA II
AE1
Pendrin
Rhcg
Cortex
CCD
Inner Medulla
IMCD
Medulla
G
H
G'
H'
I
J
I'
J'
K
L
M
N

Fig. S6

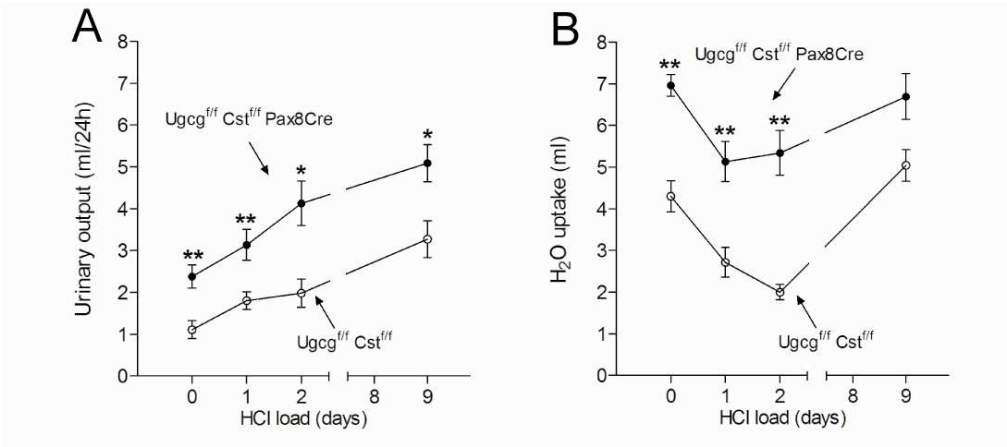
A
Urinary output (ml/24h)
Ugcg f/f Cst f/f Pax8Cre
Ugcg f/f Cst f/f
HCl load (days)
B
H2O uptake (ml)
Ugcg f/f Cst f/f Pax8Cre
Ugcg f/f Cst f/f
HCl load (days)

Fig. S7

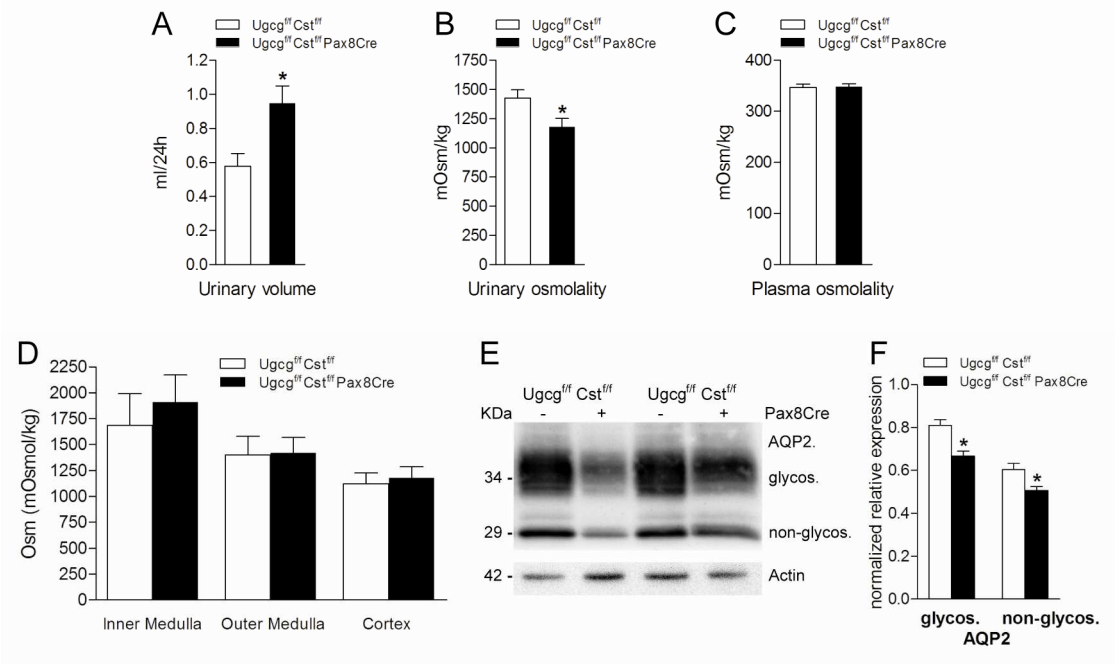
A
Ugcg^f/f Cst^f/f
Ugcg^f/f Cst^f/f Pax8Cre
ml/24h
Urinary volume
B
mOsm/kg
Urinary osmolality
C
mOsm/kg
Plasma osmolality
D
Osm (mOsmol/kg)
Inner Medulla
Outer Medulla
Cortex
E
KDa
Pax8Cre
AQP2.
glycos.
non-glycos.
Actin
34 -
29 -
42 -
F
normalized relative expression
glycos.
non-glycos.
AQP2

Fig. S8

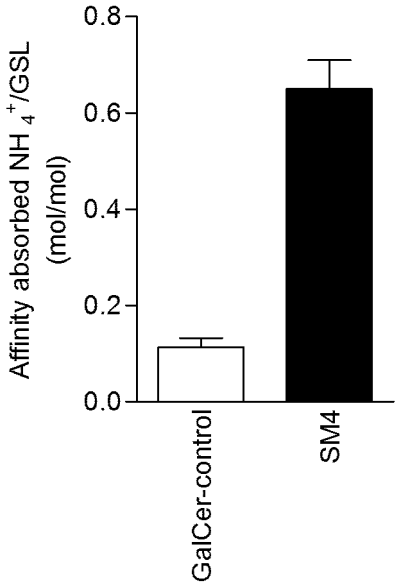
Affinity absorbed NH 4 +/GSL
(mol/mol)
0.8
0.6
0.4
0.2
0.0
GalCer-control
SM4

Fig. S9

Fig. S1. (*A-F*) Pax8-mediated β-galactosidase expression in the adult mouse kidney. (*B-F*) Enzymatic X-gal staining of cryosections of kidneys derived from R26R/Pax8^{Cre} mice was performed as described in the Methods. (*A*) A kidney from a R26R/Pax8^{cre} negative animal was taken as negative control. (*B-F*) β-galactosidase positivity was found prominently in renal tubular epithelial cells including cortical, medullary, and papillary regions. (*B* and *C*). Blood vessels were negative. (*D*) Parietal and visceral epithelial cells of glomeruli as well as thyroid gland were slightly stained. B, blood vessel; c, cortex; g, glomerulus; im, inner medulla; om, outer medulla; p, papilla.
(*G*) Southern Blot demonstrated the presence of the *Ugcg* and *Cst* null allele in kidney cortex and medulla as well as to a slight degree in thyroid of *Ugcg*$^{f/f}$ *Cst*$^{f/f}$ Pax8Cre mice.
(*H* and *I*) Sphingomyelin (SM) - and sulfatide synthesis in kidneys from *Ugcg*$^{f/f}$-, *Cst*$^{f/f}$-, and *Ugcg*$^{f/f}$ *Cst*$^{f/f}$ Pax8Cre mouse. (*H*) Thin layer chromatography (TLC) detecting SM, which appeared essentially unaltered in mutant mice. Instead, GalCer and Gal_2Cer, which were not affected by the gene deletion, accumulated significantly (Fig. 1*C*). (*I*) TLC-Immuno-overlay with sulfatide antibody. Acidic extracts of *Ugcg*$^{f/f}$-, *Cst*$^{f/f}$-, and *Ugcg*$^{f/f}$ *Cst*$^{f/f}$ Pax8Cre mouse kidneys were analyzed. Synthesis of complex sulfatides SM3 and SB1a was affected by genetic disruption of *Ugcg* as well as *Cst* whereas the GalCer derived SM4s was only affected by *Cst* disruption (see also Fig 1*A*).
(*J*) TLC of acidic GSL exctracts from cortical, medullary, and papillary tissue in wildtype mouse. Concentrations of SM3 were highest in the papilla. For abbreviations see IUPAC-IUB nomenclature of glycolipids (1999) *J Mol Biol* 286(3):963-970.

Fig. S2. *Ugcg*$^{f/f}$ *Cst*$^{f/f}$ Pax8Cre mice showed a regular renal morphology as indicated by light microscopy of paraffin sections and electron microscopy. (*A/A'* and *B/B'*) renal cortex. (*C/C'* and *D/D'*) medullary region, PAS-staining. Ultra structure of proximal tubules (*E* and *F*) as well as collecting ducts (*G* and *H*) was normal in *Ugcg*/*Cst*-deficient- (*F* and *H*) as compared to control mouse kidneys (*E* and *G*); bb, brush border membrane.

Fig. S3. Body weight (BW) at baseline and during acid loading in *Ugcg*/*Cst*-deficient mice. Renal *Ugcg*/*Cst*-deficient mice had a significant reduction of their initial BW after chronic HCl loading. The number of mice in each group is indicated in parentheses (mean ± SEM; * $P < 0.05$).

Fig. S4. Blood parameters, urinary pH, urinary ammonium, renal glutaminase activity after chronic acid load, and ammoniagenesis on isolated proximal tubules. Only mice with complete renal sulfatide deficiency showed metabolic acidosis accompanied with reduced

ammonium excretion. (*A*) blood pH; (*B*) blood bicarbonate; (*C*) blood chloride; (*D*) urinary pH; (*E*) ammonuria. The renal glutaminase activity was similar in all mutant mouse groups as compared to their control littermates, respectively (*F*). (n = 5 in $Ugcg^{f/f}$ vs. n = 5 in $Ugcg^{f/f}$ Pax8Cre; n = 7 in $Cst^{f/f}$ vs. n = 6 in $Cst^{f/f}$ Pax8Cre; n = 14 in $Ugcg^{f/f}$ $Cst^{f/f}$ vs. n = 11 in $Ugcg^{f/f}$ $Cst^{f/f}$ Pax8Cre mice - pooled from two independent experiments); (mean ± SEM; * $P < 0.05$; ** $P < 0.01$; *** $P < 0.001$).

(*G*) Ammonium production from glutamine by isolated cortical proximal tubular (PT) segments. Ammonium levels in the supernatant of $Ugcg^{f/f}$ $Cst^{f/f}$ Pax8Cre PTs increased similarly as in control PTs dependent on the time of exposure (n = 5 in $Ugcg^{f/f}$ $Cst^{f/f}$ vs. n = 3 in $Ugcg^{f/f}$ $Cst^{f/f}$ Pax8Cre mice). Note, incubations of control- or mutant PTs without glutamine resulted in very low ammonium production at the detection limit as described (1).

Fig. S5. NHE-3 mRNA levels and apical total NHE activity in kidneys from 9 days acid loaded renal *Ugcg*/*Cst*-deficient mice.

(*A*) Messenger RNA was isolated from whole kidneys of mice (n = 5 animals per genotype) and analyzed by real-time RT-PCR for NHE-3 (mean ± SEM). (*B*) Brush border membrane vesicles (BBMV) were isolated and total NHE activity was measured by the acridine orange quenching method as described in the Material and Methods. NHE activity was calculated as ratio of ΔpH (measured by the change in emission at 530 nm; Fu, fluorescence units) per min over Q, where Q is the initial quenching of fluorescence after injection of BBMV. Means ± SEM. n = 5 mice per genotype.

Fig. S6. Distal acid-base transporter- and carbonic anhydrase II mRNA expression in renal *Ugcg*/*Cst*-deficient mice.

ATPase subunits V1B1 and V0a4 excrete protons into collecting duct (CD) lumen; cytosolic CA II catalyzes generation of bicarbonate which is subsequently secreted by the type - A IC specific basolateral chloride/bicarbonate exchanger AE1 (anion exchanger-1). The non-type-A IC specific luminal anion exchanger pendrin is critical for urinary bicarbonate secretion and reabsorption of chloride. CD ammonia secretion is mostly mediated by the Rhcg ammonia transporter (2). Mice (n = 5 or 6 per genotype) were exposed to an HCl load for 9 days, kidneys were excised, and mRNA levels of respective genes were analyzed by real-time RT-PCR. (A) V1B1 ATPase subunit; (*B*) V0a4 ATPase subunit; (*C*) CA II; (*D*) AE1; (*E*) Pendrin; (*F*) Rhcg. Data are presented as mean ± SEM.

(*G-J*) Immunofluorescence of the V-ATPase subunit V1B1. Kidney sections of 9 days acid loaded renal Ugcg/Cst-deficient- and control mice were costained with the V1B1 subunit

(green) and the principal cell-specific AQP2 channel (red). Nuclei were detected using DAPI staining. No obvious alterations in intensity and subcellular localization were seen. Representative kidney sections from 9 days acid loaded Ugcg/Cst- and control kidneys (n = 5 per genotype) are shown; scale bars = 100 µm. (*G* and *H*) CCD (cortical collecting duct); (*I* and *J*) IMCD (inner medullary collecting duct). *G*'/*H*' and *I*'/*J*' are higher magnifications of *G*/*H* and *I*/*J*.

(*K*-*N*) Rhcg immunofluoresence staining in cortex (*K* and *L*) and outer medulla (inner stripe) (*M* and *N*). Representative kidney sections from 9 days acid loaded *Ugcg*/*Cst*- and control kidneys (*n* = 5 per genotype) are shown; scale bars = 100 µm.

Fig. S7. Urinary output and water uptake at baseline and during acid loading in *Ugcg*/*Cst*-deficient mice.

(*A*) Renal *Ugcg*/*Cst*-deficient mice showed increased urinary output (*n* = 5 - 7) as compared to control littermates (*n* = 7 - 9). (*B*) Polydipsia occurred in renal *Ugcg*/*Cst*-deficient mice as compared to control littermates (*n* = 5 or 6 per genotype); data for (*A*) and (*B*) are presented as mean ± SEM (* $P < 0.05$; ** $P < 0.01$).

Fig. S8. Renal water handling and osmoregulation after 24 hr thirst in *Ugcg*/*Cst*-deficient mice.

Control- and renal *Ugcg*/*Cst*-deficient mice (*n* = 5 or 6 per genotype) were placed in metabolic cages under dehydrated conditions and 24 h urine was collected. (*A*) urinary output urinary; (*B*) urinary osmolality; (*C*) plasma osmolality. Means ± SEM (* $P < 0.05$).

(*D*) Osmolality in cortical, outer medullary, and inner medullary tissue (*n* = 7 in control; *n* = 9 in renal *Ugcg*/*Cst*-deficient mice).

(*E* and *F*) Western blot analysis of the distal water channel AQP2. (*E*) Membrane proteins from kidneys (*n* = 4 per genotype) probed with AQP2 antibody detecting the glycosylated and non-glycosylated protein. Two representative membrane protein samples per genotype are shown. (*F*) Densitometric evaluation. (Means ± SEM. * $P < 0.05$).

Fig. S9. Ammonium binding to SM4.

SM4-sepharose affinity column was able to absorb NH_4^+ in an almost equimolar range, whereas galactosylceramide (GalCer)-sepharose only marginally binds NH_4^+. The experiment was repeated twice with similar results.

SUPPORTING TABLES AND TABLE LEGENDS

Tab. S1.

Ugcg$^{f/f}$ Cst$^{f/f}$	*Pax8Cre -*	*Pax8Cre +*
Body weight (g)	21.1 ± 0.8 (9)	20.7 ± 0.4 (7)
Kidney weight (mg/g BW)	5.5 ± 0.2 (6)	4.9 ± 0.1 (6)*
Food intake (mg/24 h/g BW)	0.18 ± 0.01 (9)	0.18 ± 0.02 (6)
Water uptake (ml/24 h/g BW)	0.22 ± 0.02 (7)	0.35 ± 0.02 (6)**
Blood values		
Plasma creatinine (mg/dl)†	0.13 ± 0.01 (5)	0.14 ± 0.01 (6)
pH	7.37 ± 0.01 (9)	7.39 ± 0.01 (7)
pCO_2 (mmHg)	36.4 ± 1.3 (9)	35.7 ± 1.6 (7)
HCO_3^- (mmol/l)	20.3 ± 0.8 (9)	21.1 ± 1.0 (7)
K^+ (mmol/l)	3.78 ± 0.1 (9)	3.67 ± 0.12 (7)
Na^+ (mmol/l)	143.5 ± 0.3 (9)	143.7 ± 0.8 (7)
Calcium (mmol/l)	1.21 ± 0.01 (9)	1.23 ± 0.02 (7)
Cl^- (mmol/l)	110.8 ± 0.6 (9)	111.3 ± 0.3 (7)
Serum fT4 (pg/ml)	10.3 ± 4.7 (4)	14.7 ± 3.9 (4)
Crea Clearance (µl/min/g BW)†	4.7 ± 0.7 (5)	4.6 ± 0.8 (6)
Urinary values		
Volumen (ml/24 h)	1.11 ± 0.21 (9)	2.38 ± 0.28 (7)**
Creatinine (µM/24 h)	5.9 ± 0.6 (9)	6.0 ± 0.6 (7)
Na^+ (mM mM^{-1} creat.)	19.5 ± 1.3 (9)	22.8 ± 1.0 (7)
K^+ (mM mM^{-1} creat.)	16.4 ± 1.9 (8)	40.1 ± 4.9 (5)**
Cl^- (mM mM^{-1} creat.)	451.1 ± 44.7 (8)	265 ± 67.7 (7)
Ammonium (mM mM^{-1} creat.)	13.6 ± 1.1 (15)	7.8 ± 0.9 (15)**
TA (mEq mM^{-1} creat.)	18.7 ± 3.0 (8)	38.8 ± 2.2 (6)**
NAE (mEq mM^{-1} creat.)	33.1 ± 2.2 (6)	52.1 ± 7.0 (5)**

Tab. S2.

	Day 2		**Day 9**	
Ugcg$^{f/f}$ *Cst*$^{f/f}$	*Pax8Cre -*	*Pax8Cre +*	*Pax8Cre -*	*Pax8Cre +*
Body weight (g)	18.9 ± 0.7 (9)^{A}	18.5 ± 0.4 (7)^{B}	18.6 ± 0.5 (14)^{A}	17.6 ± 0.5 (11)^{B}
Food intake (mg/d/g BW)	0.37 ± 0.02 (9)^{B}	0.35 ± 0.02 (6)^{B}	0.48 ± 0.02 (14)^{C}	0.47 ± 0.02 (11)^{B}
Water uptake (ml/d/g BW)	0.15 ± 0.02 (7)	0.29 ± 0.03 (7)**	0.23 ± 0.02 (11)	0.36 ± 0.03 (10)**
Blood values	*n = 9*	*n = 6*	*n = 13-14*	*n = 12*
pH	7.16 ± 0.03^{C}	7.09 ± 0.03^{B}	7.21 ± 0.03^{C}	7.05 ± 0.04*^{C}
pCO_2 (mmHg)	31.9 ± 34.3^{A}	34.3 ± 1.2	39.3 ± 1.3	39.1 ± 1.6
HCO_3^- (mmol/l)	11.1 ± 0.7^{C}	10.0 ± 0.5^{B}	15.2 ± 1.1^{B}	10.7 ± 1.2* ^{C}
K^+ (mmol/l)	3.96 ± 0.14	4.23 ± 0.19^{A}	4.05 ± 0.12	4.18 ± 0.13^{A}
Na^+ (mmol/l)	148.5 ± 1.2^{B}	148.2 ± 0.5^{B}	148.4 ± 0.8^{C}	152.5 ± 0.7**^{C}
Calcium (mmol/l)	1.36 ± 0.01^{C}	1.39 ± 0.01^{B}	1.34 ± 0.02^{C}	1.40 ± 0.03^{B} *
Cl^- (mmol/l)	124.1 ± 0.9^{C}	126.8 ± 0.7^{B}	119.9 ± 1.3^{C}	128.4 ± 1.3***^{C}

Tab. S3.

Ugcg$^{f/f}$ *Cst*$^{f/f}$	*Pax8Cre* -	*Pax8Cre* +
	CCD (n = 7)	CCD (n = 7)
Tubule length, mm	0.33 ± 0.04	0.52 ± 0.09
Tubule diameter, µm	49.37 ± 4.36	59.44 ± 4.89
Area (mm^2)	0.52 ± 0.08	1.03 ± 0.25
Collection rate, $nl \cdot mm^{-1} \cdot min^{-1}$	17.32 ± 2.15	12.70 ± 2.68
Perfusate pH	6.39 ± 0.03	6.37 ± 0.03
End-luminal pH	6.39 ± 0.03	6.37 ± 0.03
Bath pH	7.40±0.02	7.41±0.02
Total ammonia perfusate, mM	1.79 ± 0.05	1.80 ± 0.10
[NH_3] perfusate, µM	4.15 ± 0.35	3.95 ± 0.24
Total ammonia bath, mM	1.79 ± 0.05	1.80 ± 0.10
[NH_3] bath, µM	41.78 ± 2.66	42.90 ± 2.66
Total ammonia collected, mM	3.71 ± 0.41	4.45 ± 0.63
[NH_3] collected, µM	8.76 ± 1.30	9.73 ± 1.22
Total ammonia flux, $pmol \cdot mm^{-1} \cdot min^{-1}$	-28.89 ± 4.56	-27.18 ± 3.53
NH_3 permeability, cm/s	0.009 ± 0.001	0.008 ± 0.002

Tab. S1. Basic physiological parameters in renal *Ugcg*/*Cst*-deficient and control mice (females, 3 months old). Numbers of mice are indicated in parentheses. Urine and blood samples were collected and analyzed as described in the Supporting Methods. †Creatinine clearance was obtained when food was withheld during 24 h urine collection, drinking water was freely available, as described in the Supplemental Experimental Procedures.

Crea = creatinine; fT4 = free thyroxin 4; TA = titratable acids; NAE = Net acid excretion. Means ± SEM; * $P < 0.05$; ** $P < 0.01$.

Tab. S2. Blood parameters in renal *Ugcg*/*Cst*-deficient- and control mice exposed to an acute and chronic acid load.

Means ± SEM; asterisks indicate significance versus controls on the same day (* $P < 0.05$; ** $P < 0.01$; *** $P < 0.001$); letters indicate significance versus baseline in same genotype (^{A} $P < 0.05$; ^{B} $P < 0.01$; ^{C} $P < 0.001$).

Tab. S3. Physical parameter of *in vitro* microperfused CCDs.

Values are mean ± SEM; *n,* number of mice; CCD, cortical collecting duct.

SUPPORTING MATERIALS AND METHODS

β-Galactosidase (lacZ) staining on cryosections. Pax8Cre were mated with homozygous Rosa26 Cre reporter mice. Animals positive for both R26R and Pax8Cre were used to monitor Pax8 driven Cre recombinase activity. Littermates positive for R26R and negative for Pax8Cre were taken as controls. R26R/Ugcg$^{f/+}$//Cst$^{f/+}$ Pax8Cre- and control mice were sacrificed by cervical dislocation. Organs were quickly removed, embedded in tissue tek® (Sakura Labortechnik) while freezing on dry ice and stored at -80°C. 5 µm coronal cryosections were made and collected in two series for β-galactosidase and H&E staining. Sections were fixed in 1% PFA for 15 min at RT. Sections were washed twice with X-Gal washing buffer and then incubated with X-Gal staining solution for 3 h at 37°C. Then, sections were mounted with FluoroMount and viewed through a light microscope.

Generation of mice with loxP flanked *Gal3st1* (*Cst*) gene. All three splice variants of the *Cst* gene consist of two identical coding exons designated in the present manuscript coding exon1 and 2 (CE1 and CE2). The *Cst*-targeting vector was assembled in a pBluescript plasmid (Stratagene, La Jolla, CA, USA) (Figure 1B). One 4.5kb Nhe I/Sst II fragment including the coding exon CE1 and part of CE2 of the *Cst* gene was subcloned from a mouse Bac-library (German Resource Center (RZPD), Berlin, Germany) into pBluescript modified with a Nhe I site 5 prime of the multiple cloning site (MCS). A neomycin resistance cassette flanked by two FRT sites and with a loxP site at the 5 prime end of the resistance cassette was inserted into Hind III of the 4.5kb fragment. A second 3.5 kb genomic fragment obtained by Nhe I/Sst II restriction digest containing the residual part of CE2 was inserted into Sst II/Spe I of the MCS of the modified pBluescript plasmid. Thereby, the Nhe I-site of of the Cst 3.5 kb fragment was eliminated. A single loxP site with a 3'-diagnostic Sca I restriction site was inserted into the Nde I restriction site and a PGK-DTA cassette was inserted 3 prime of the genomic sequence into Cla I/Kpn I of the 3.5kb fragment. In addition a Nhe I site was inserted 5-prime into the MCS of the vector containing the Cst 3.5 kb fragment. The plasmids containing the 4.5kb and 3.5kb *Cst* fragments were digested with Nhe I/Sst II and the liberated 4.5kb fragment inserted into the 3.5kb fragment containing vector. The targeting construct was linearized with Nhe I. E14 ES-cells derived from mouse strain 129 SV Ola were transfected in the presence of the *Cst*-targeting construct. Stem cell clones were picked, expanded and checked for homologous recombination of *Cst*. As verified by southern blot analysis and PCR, in 3 out of 192 clones homologous integration of the complete construct was achieved. Germline transmission of mutant stem cells was indicated by agouti colored

offspring from chimeras. F1-offspring with loxP-flanked exon 3 were further mated with FLP-deleter mice (3) to obtain the floxed *Cst* gene without neomycin cassette. Mice were backcrossed for at least 7 generations into C57Bl6 background.

Generation of *Ugcg*$^{f/f}$-, *Cst*$^{f/f}$-, and *Ugcg*$^{f/f}$ *Cst*$^{f/f}$ Pax8Cre mice. Mice with loxP flanked gene *Ugcg* encoding the enzyme UDP-glucose-ceramide glucosyltransferase (*Ugcg*$^{f/f}$) were generated and genotyped as described earlier (4). Mice with deletions of *Cst*- and *Ugcg* gene specifically in the kidney were generated by crossing *Cst*- or *Ugcg* floxed mice, respectively, with mice expressing the cre-recombinase under control of the Pax8 promoter (5). Double mutant *Ugcg*$^{f/f}$ *Cst*$^{f/f}$ Pax8Cre mice were generated by crossing *Cst*- and *Ugcg* floxed mice with each other and with Pax8Cre mice. Mice were kept under specific pathogen-free conditions in barrier facilities in groups up to 5 animals per cage. If not otherwise noted, animals had free access to standard laboratory chow (Provimi Kliba Nafag, #3437) and drinking water.

Genotyping of mutant and control mice was performed by PCR analysis of genomic DNA obtained from tail biopsies using following primers:

Cst-wild-type forward: 5'-tggtacctccactgtatcccaaca-3';

wild-type/*Cst*-flox reversed: 5'-ccagcaagtcccttaggagtcaga-3';

Pax8 forward: 5'-tgtccctgacaatttggtctgtt-3'; Pax8-*cre* reverse: 5'-ggaaaccatttccggttattcaa-3'.

PCR products of 147 bp and 268 bp indicated the *Cst* wild type and floxed allele, respectively; a PCR product of 600 bp indicated the Pax8Cre transgene. Primers used to verify the *Ugcg*-floxed gene have been described before (4).

Southern Blot Analysis was performed after digestion of isolated DNA from tissue samples from organs with the restriction enzymes Bgl II (for *Ugcg*) and Sca I (for *Cst*) using the PCR DIG Probe Synthesis Kit and DIG Luminescent Detection Kit (Roche, Mannheim, Germany; DIG, digoxigenin) according to the manufacturer's instructions. The primers used to synthesize the Cst Southern probe were:

5' probe forward: 5'-gctacgagaatcttcatccctcta-3'; reversed: 5'-ctgggaatctgtgtctcatctgta-3';

3' probe forward: 5'-gcctcaacccttagttcttattcat-3'; reversed: 5'-ggactggattacttggtcagtctt-3'.

Primers used to synthesize the Ugcg Southern probe have been described (4).

GSL extraction. Mice were sacrificed by cervical dislocation and kidneys were rapidly dissected. Whole kidneys or dissected cortical, medullary, and papillary tissue, respectively, were snap-frozen in liquid nitrogen and stored at -80°C. GSLs were extracted according to Sandhoff with modifications (6). Frozen tissue was lyophilized (Alpha 1-2 Lyophilizer,

Christ, Germany) overnight. The dried tissue was weighed, manually powered, and extracted for GSLs twice with 2 ml of $CHCl_3/CH_3OH/H_2O$ (C/M/W) 10:10:1(v/v/v) and with 2 ml of C/M/W 30:60:8 (v/v/v). Each time, samples were sonicated at 50°C for 15 min and subsequently centrifuged (2500 x *g*, 10 min, RT). Pooled supernatants were dried in an evaporator at 37°C under a stream of air. In order to remove phospholipids and triglycerides, the dried GSL extracts were subjected to mild alkaline hydrolysis (1 ml of 0.1 M KOH in CH_3OH, 50°C, 4 h). Then, GSL exctracts were neutralized by addition of acetic acid and samples were dried in an evaporator. Samples were desalted by reversed phase (RP)-18 column chromatography (Porasil silica 125 Å 55-105 µm, Waters, USA), and GSLs were eluted with methanol and dried.

Neutral and acidic GSLs were separated using diethylaminoethyl (DEAE) - Sephadex A-25 (Pharmacia Biotech, Sweden) chromatography. Briefly, neutral GSL fraction was eluted with C/M/W 30:60:8 (v/v/v) and acidic GSLs were eluted with 0.5 M potassium acetate (KAc) in methanol and thereafter desalted again by RP-18 column chromatography. The neutral GSL fraction was further purified after peracetylation of the sugar OH-groups. Peracetylated nGSLs were eluted with 4 ml of DCE/acetone 1/1 (v/v), deacetylated by subjection to mild alkaline hydrolysis and subsequently desalted by RP-18 chromatography. Aliquots corresponding to 4 mg of whole or dissected cortical, medullary, and papillary tissue kidneys were spotted on TLC plates (HPTLC plates, silica gel 60 F254, Merck, Germany). After a pre-run with chloroform/aceton 1:1 (v/v), neutral GSLs were separated by running the TLC in C/M/W 62.5:30:6 (v/v/v) and acidic GSLs were separated using running solvent C/M/0.2% aqueous $CaCl_2$ 60:35:8 (v/v/v). Bands were detected using orcinol/sulfuric acid spray reagent (0.2% orcinol in 10% sulfuric acid) and exposure at 120°C for 10 min.

TLC immuno-overlay. Acidic GSL extracted from kidneys of mutant and control mice and a sulfatide standard containing murine sulfatides SM4s, SM3, and SB1a were separated by TLC as described. The dried plate was overlayed with a plexigum solution (5% polyisobutyl-methacrylate, Sigma-Aldrich, Germany; dissolved in chloroform and diluted 1:10 with n-hexane), and incubated at RT for 2 min. Unspecific binding sites were blocked with 1% BSA in PBS for 1 h at RT and the plate was incubated with an affinity purified mouse antibody specifically detecting sulfated GSLs (monoclonal mouse IgG raised in *Cst* null mice, 1:50 in 1% BSA in PBS, kindly provided by H.-W. Zentgraf, Heidelberg) at 4°C overnight. After washing with PBS/0.05% Tween-20, the plate was incubated with secondary horseradish-peroxidase linked goat-α-mouse (1:500 in 1%BSA in PBS) for 2 h at RT. After 3 times of

washing, antibody was detected using Sigma Fast BCIP (Sigma, Germany). Plexigum and Sigma Fast staining were removed with acetone and GSLs including sulfatides were detected with orcinol.

Measurement of urinary pH and creatinine clearance. Mice were individually placed in mouse-specific metabolic cages (Phymep S.A.R.L., Paris, France) in a temperature and light controlled room, with drinking water freely available; food was withheld. After adaption to the cages (3 days for 3 h each), urine was collected for 24 hours under mineral oil. Body weight, urine volume, and water consumption of mice was monitored. Immediately after the experiment, blood was collected from the ophthalmic venous plexus of anesthetized mice. Blood samples were centrifugated at 5000 x *g* for 5 min to obtain plasma; urine samples were centrifugated at 3000 x *g* for 5 min to get rid of precipitates. Urinary pH was measured immediately using a pH-microelectrode (691 pH meter, Metrohm, Switzerland). Urinary and plasma creatinine for calculation of the creatinine clearance was determined by an enzymatic assay (Crea-Plus kit, Roche, Germany).

Acid-loading. Mice were individually placed in mouse-specific metabolic cages (Tecniplast, Buguggiate, Italy) in a temperature- and light controlled room. Mice were allowed to adapt to cages for 1 day before urine collections. They had free access to drinking water and standard chow. Urine was collected for 24 h under mineral oil for two consecutive intervals. Daily chow and water intake were measured; urine volume and body weight were monitored. Then, a 3:2 mixture (vol/wt) of 0.3 M HCl and powdered standard chow (GLP3433, Kliba AG, Switzerland) was given for 9 days. Urine was collected after 1, 2, and 9 days of acid-loading as described for the standard diet. Blood was taken under standard diet and after 2 and 9 days of acid-loading. Mice were anesthetized with isoflurane (2%) and blood was collected with a blood gas capillary from the ophthalmic venous plexus. Blood and urine samples were measured for pH, blood gases, and electrolytes on a Radiometer ABL 815 Flex blood gas analyzer (Copenhagen, Denmark). Urinary pH was also measured using a pH-microlelectrode (691 pH meter, Metrohm, Switzerland). Urinary NH_3/NH_4^+ and creatinine were assessed using the method of Berthelot (7) and Jaffé (8), respectively. TA were determined according to Chan (9). Urinary bicarbonate was calculated from urinary pH and PCO_2. NAE was calculated as (NH_4^+ + TA) - bicarbonate, expressed as mEq.

Glutaminase activity determination. Glutaminase was measured using a two step assay as described (10, 11).

Determination of ammonium production by isolated proximal tubule (PT) segments. Renal cortices were dissected from both kidneys, treated with collagenase and trypsin inhibitor, and PTs were collected as described (12). The remaining PT fragments were resuspended in Krebs-Henseleit bicarbonate (KHB) buffer pH 7.4, gassed for at least 30 min with 95% O_2/5% CO_2 (1). Ammonium production by isolated PTs from control and double mutant *Ugcg*$^{f/f}$ *Cst*$^{f/f}$ Pax8Cre mice was measured in absence or presence of 10mM glutamin in 5ml Krebs-Henseleit buffer as described (1). Ammonium production has been related to protein content of isolated PTs, respectively.

Thirst experiment. Urine and plasma samples were obtained as described for determination of plasma and urinary creatinine except of water and food was withheld for 24 h. Osmolality was measured.

Measurement of serum free T4.

Blood was collected from the ophthalmic venous plexus of anesthetized mice. Then, blood samples were allowed to clot by RT for 30 min. Blood samples were centrifugated at 5000 x *g* for 5 min to obtain serum. Measurement of serum free thyroxin 4 was carried out using an ELISA assay (Alpha Diagnostics Int., San Antonio, USA) according to the manufacturer's guidelines.

Real-time RT-PCR. Total RNA was extracted according to the method of Chomczynski and Sacchi (13). Genomic DNA was removed using the TURBO DNA-free™ Kit (Ambion). RNA quality was tested using the RNA 6000 Nanochip (Agilent Technologies) and the 2100 Bioanalyzer (Agilent Technologies). RNA was reverse transcribed into cDNA using SuperScript™ II First Strand System (Invitrogen, Germany). Messenger RNA expression of target genes was analyzed by quantitative Real-time PCR using the LightCycler® 2.0 System and the LightCyler FastStart® DNA MasterSYBR Green I kit (Roche Diagnostics, Mannheim, Diagnostics) according to the manufacturer's instructions. The comparative cycle threshold method was applied to evaluate the fluorescence values (14). Ct values of *Ugcg*$^{f/f}$ *Cst*$^{f/f}$ Pax8Cre and control mice were obtained. Ribosomal 18s rRNA was used as housekeeping gene and relative target gene expression was calculated according to the $2^{-\Delta\Delta Ct}$ formula. Primer sequences used for amplification of SNAT3, PEPCK, phosphate dependent GA, Carbonic anhydrase, and Pendrin are described in (15). Primer sequences for NHE-4, NKCC2, NHE-3, AE1, ATP6V0a4, ATP6V1B1; NBCn1 are described in (16-18). Primers used (forward and reverse) for Rhcg (NM_019799) and 18S rRNA were:

Rhcg: 5´-gttggagaagaagcgcaagaa-3´; 5´-cgaagaccatggcgtgtaca-3´,

18srRNA: 5´-tgccctatcaactttcgatggta-3´; 5´-caattacagggcctccaaagagt-3´.
The appropriate amplification conditions for the LightCycler® 2.0 System were tested for each primer pair and amplification of the correct product was assured by gel electrophoresis.
Western Blotting. A small slice of frozen kidney tissue was put in ice-cold HEPES lysis buffer (20 mM HEPES buffer, pH 7.4, 25 mM KCl, 250 mM sucrose, 2 mM $MgCl_2$) containing 1x protease inhibitor cocktail (Complete, Roche) and 0.5 mM PMSF. Homogenization was performed on ice using the Ultra Turrax® T25 basic power homogenizer at 22,000 rpm and cell debris were subsequently centrifuged at 1000 x *g* for 20 min at 4°C. The supernatant was centrifuged at 100,000 x *g* for 1 h at 4°C in a table ultracentrifuge (TLS 55, Beckman swinging bucket rotor). Supernatant containing the cytoplasmic fraction was taken off. Pellet containing membrane protein was resolved in ice-cold HEPES lysis buffer containing 1% digitonin. Membrane pellets were dissolved using a sonicator (Branson) and samples were stored in aliquots at -80°C. Protein concentration was determined by the Bradford method (19). Protein samples were denaturated by adding 4x Laemmli sample buffer containing 8% SDS and heating at 96°C for 5 min. 30-50 µg of membrane or cytoplasmic protein were separated on 10% polyacrylamide gels by SDS-PAGE and subsequently transferred electrophoretically to nitrocellulose membranes (3-4 h, at 180 mA). Non-specific protein binding sites on membranes were blocked with 5% milk for 1 h at RT and blots were incubated with primary antibodies overnight at 4°C. β-actin was used as a reference protein. Membranes were washed with PBS/0.1% Tween 20 (3 times for 10 min) and subsequently incubated for 1 h at RT with secondary antibodies. After washing the membrane, antibody binding was detected using chemiluminescence substrate (Amersham ECL, GE Healthcare) followed by exposure to X-ray film (Amersham Hyperfilm ECL, GE Healthcare). Molecular weight of proteins was juged from a PageRuler™ prestained protein ladder (SM 0671, Fermentas). Films were scanned (ScanMaker, Microtek, USA) and the intensities of the bands were quantified using ImageJ 1.30v. Proteins were normalized to actin. Primary antibodies used were rabbit anti-PEPCK, 1:200 (Cayman Chemical); goat anti-Glud1/2 (G-14), 1:500 (Santa Cruz); rabbit anti-KGA (kidney specific glutaminase), 1:1000 (kindly provided by N. Curthoys, Colorado); rabbit anti-NKCC2, 1:500 (Millipore); goat anti-AQP2 (C-17), 1:200 (Santa Cruz); monoclonal rabbit anti-actin (I-19), 1:2000 (Santa-Cruz). Secondary antibodies used were horseradish peroxidase-conjugated goat anti-rabbit IgG (Santa Cruz, sc-2004), and HRP-conjugated donkey anti-goat IgG (Santa Cruz, sc-2020) diluted 1:2000.

Immunofluorescence. Mice were anesthetized i.p. with tribromoethanol (avertin) and transcardially perfused with 50 ml of 4% formalin in PBS (Secure perfusion system; 99ml/h,) at RT. Kidneys were removed, transversely cut, and immersion fixed in 4% formalin overnight. Kidney tissue was embedded in paraffin and cut in 3 µm sections. After deparaffinization, an antigen retrieval step was performed by incubation of sections either in citrate buffer pH 6.0 at 98°C for 20 min in the microwave (AQP2; V1B1 ATPase subunit), or incubation in Tris buffer, pH 9.0 for 5 min in the pressure cooker (Rhcg). Then, nonspecific binding sites were blocked for 30 min with 10% fetal calf serum in PBS/0.1% Tween. Primary antibodies were diluted in antibody diluent (Dako, Germany) and applied to the sections at RT for 1 - 2 h. Negative control sections without primary antibody were incubated with 10% FCS only. After 3 washing steps with PBS/0.1% Tween20**,** sections including the negative controls were incubated in the dark for 1 h with corresponding secondary antibodies. Sections were counterstained for nuclei with DRAQ5 (Alexis, San Diego, CA) 1:5000 in PBS/0.1% Tween at RT for 10 min. After washing with aqua bidest., sections were mounted in FluoroMount G (Southern Biotech). For double immunofluorescence staining, sections were blocked again briefly with 10% FCS before applying the antibodies as described above. Images were taken with a Leica TCS SL confocal scanning system, with microscope DMRE and Leica confocal software, Version 2.61 (Leica, Wetzlar, Germany). The primary antibodies used were rabbit anti-V-ATPase subunit V1B1, 1:5000, (20); rabbit anti-Rhcg, 1:200 (kindly provided by D. Weiner, California); goat anti-AQP2 (C-17), 1:800 (Santa Cruz). The secondary antibodies used were donkey anti-goat 546 (1:200); donkey anti-rabbit 488, 1:200 (Alexa Flour®).

Ammonium binding to SM4.

2 ml of Sepharose 4B CL were coated with 2.4 µmol SM4 or galactosylceramide as described previously (21, 22). The sepharose, either GSL-coated or non-coated, was filled into small glass columns and washed with 10 ml of distilled water. Subsequently, 10 ml of 1 M NH_4Cl in water were applied to each of the columns. Columns were washed with 30 ml of water and bound ammonium was eluted with 10 ml 1 M NaCl in H_2O. An aliquot of 100 µl was used for the determination of NH_4^+ using an ammonium determination kit (Sigma) according to the manufacturer's instructions.

REFERENCES

1. Chobanian MC & Julin CM (1991) Angiotensin II stimulates ammoniagenesis in canine renal proximal tubule segments. *Am J Physiol* 260(1 Pt 2):F19-26.
2. Wagner CA, Devuyst O, Bourgeois S, & Mohebbi N (2009) Regulated acid-base transport in the collecting duct. *Pflugers Arch* 458(1):137-156.
3. Rodriguez CI*, et al.* (2000) High-efficiency deleter mice show that FLPe is an alternative to Cre-loxP. *Nat Genet* 25(2):139-140.
4. Jennemann R*, et al.* (2005) Cell-specific deletion of glucosylceramide synthase in brain leads to severe neural defects after birth. *Proc Natl Acad Sci U S A* 102(35):12459-12464.
5. Bouchard M, Souabni A, & Busslinger M (2004) Tissue-specific expression of cre recombinase from the Pax8 locus. *Genesis* 38(3):105-109.
6. Sandhoff R*, et al.* (2002) Kidney sulfatides in mouse models of inherited glycosphingolipid disorders: determination by nano-electrospray ionization tandem mass spectrometry. *J Biol Chem* 277(23):20386-20398.
7. Berthelot M (1859) Violet d'aniline. *Rep Chim App* 1:284.
8. Seaton B & Ali A (1984) Simplified manual high performance clinical chemistry methods for developing countries. *Med Lab Sci* 41(4):327-336.
9. Chan JC (1972) The rapid determination of urinary titratable acid and ammonium and evaluation of freezing as a method of preservation. *Clin Biochem* 5(2):94-98.
10. Parry DM & Brosnan JT (1978) Glutamine metabolism in the kidney during induction of, and recovery from, metabolic acidosis in the rat. *Biochem J* 174(2):387-396.
11. Kenny J*, et al.* (2003) Bacterial expression, purification, and characterization of rat kidney-type mitochondrial glutaminase. *Protein Expr Purif* 31(1):140-148.
12. Terryn S*, et al.* (2007) A primary culture of mouse proximal tubular cells, established on collagen-coated membranes. *Am J Physiol Renal Physiol* 293(2):F476-485.
13. Chomczynski P & Sacchi N (1987) Single-step method of RNA isolation by acid guanidinium thiocyanate-phenol-chloroform extraction. *Anal Biochem* 162(1):156-159.
14. Livak KJ & Schmittgen TD (2001) Analysis of relative gene expression data using real-time quantitative PCR and the 2(-Delta Delta C(T)) Method. *Methods* 25(4):402-408.

15. Nowik M, *et al.* (2008) Genome-wide gene expression profiling reveals renal genes regulated during metabolic acidosis. *Physiol Genomics* 32(3):322-334.
16. Benziane B, *et al.* (2007) NKCC2 surface expression in mammalian cells: down-regulation by novel interaction with aldolase B. *J Biol Chem* 282(46):33817-33830.
17. Bonnici B & Wagner CA (2004) Postnatal expression of transport proteins involved in acid-base transport in mouse kidney. *Pflugers Arch* 448(1):16-28.
18. Bourgeois S, *et al.* (2010) NHE4 is critical for the renal handling of ammonia in rodents. *J Clin Invest* 120(6):1895-1904.
19. Bradford MM (1976) A rapid and sensitive method for the quantitation of microgram quantities of protein utilizing the principle of protein-dye binding. *Anal Biochem* 72:248-254.
20. Wagner CA, *et al.* (2003) A rapid enzymatic method for the isolation of defined kidney tubule fragments from mouse. *Pflugers Arch* 446(5):623-632.
21. Nores GA, Dennis RD, Helling F, & Wiegandt H (1991) Human heterophile antibodies recognizing epitopes present on insect glycolipids. *J Biochem* 110(1):1-8.
22. Jennemann R, Sandhoff R, Grone HJ, & Wiegandt H (2001) Human heterophile antibodies recognizing distinct carbohydrate epitopes on basidiolipids from different mushrooms. *Immunol Invest* 30(2):115-129.